

EFFECT OF MICROCRACKING ON GAS PERMEABILITY AND CHLORIDE DIFFUSION OF CONCRETE

A. DJERBI TEGGUER^{*}, S. BONNET[†], A. KHELIDJ[†] AND V. BAROGHEL-BOUNY^{*}

^{*} Institut français des sciences et technologies des transports, de l'aménagement et des réseaux (IFSTTAR),
58 Bd Lefebvre, F-75732, Paris Cedex 15, France
e-mail: assia.tegguer@ifsttar.fr, web page: <http://www.ifsttar.fr>

[†] Institut de Recherche en Génie Civil et Mécanique IUT de Saint-Nazaire (GeM (UMR CNRS 6183))
58 rue Michel Ange, B.P. 420, F-44606 Saint-Nazaire Cedex- France
e-mail: bonnet-s@univ-nantes.fr, web page: <http://gem.ec-nantes.fr>

Key words: Crack, Diffuse damage, Chloride Diffusion, Durability, Gas Permeability, High performance concrete, Time lag.

Abstract: Concrete structures near marine environments are subjected to a combination of chloride and varying stress conditions resulting in both macro and microcracking. Knowledge of the transport properties of cracked concrete is essential for predicting its durability. The impact of damage upon gas permeability and chloride diffusion through ordinary concrete (OC) and high performance concrete (HPC) was carried by an experiment in the present study. Concrete cylinders were induced microcracks by mechanical uniaxial compression between 60% and 90% of the ultimate strength. The damage of specimens was evaluated by elastic stiffness degradation and ultrasound pulse velocity. After unloading intrinsic gas permeability was measured using a constant head permeameter, the chloride migration coefficient was evaluated by migration test in steady state conditions, with the same concrete specimen. The damage of specimens showed correlation with gas permeability and chloride diffusion of concrete in this experiment. A linear correlation was obtained between intrinsic permeability coefficient and chloride diffusion coefficient depending on the damage variable, specific for each concrete type (OC and HPC).

1 INTRODUCTION

Understanding transport phenomena in concrete at its microstructural level has become of increasing importance in elucidating the deterioration process of concrete such as corrosion of reinforcement embedded in concrete which is caused by penetration of aggressive substances into concrete. Concrete structures near marine environments are subjected to a combination of chloride and load. The chloride resistance of concrete is governed primarily by the pore structure and the concrete diffusivity. The corrosion onset is dependent on the concrete

permeability (Oxygen transport) [1] and on the thickness of concrete cover.

Extensive work has been carried on over the past decades to understand transport properties of concrete, and numerous service life prediction models have been introduced. The disadvantage of these models is that all predictions are carried out considering a perfect, uncracked concrete [2-4]. Concrete structures in service are subjected to varying stress conditions resulting in both macro and microcracking. Knowledge of the transport properties of cracked concrete is essential for predicting its durability. The presence of cracks can significantly modify transport

properties of concrete. Microcracks that are discrete and well distributed will influence transport in very different manner compared to visible connected localized macrocracks. Transport in a cracked concrete is corresponding to a coupled phenomenon between transport into the matrix and the crack. However, since the kinetics of different transport process varies, changes resulting from cracking greatly depend on the mechanism which is predominant [5-17].

In the case of localized damage it has been shown that gas permeability of concrete measured on disks fractured using a splitting tensile test increases with crack opening displacement COD cubed [5]. Concerning chloride diffusion measured by migration test, a linear variation was obtained between the diffusion coefficient through the crack and crack width, this coefficient was not dependent on material parameters and becomes constant when the crack width was higher than 80 μm , its value is the diffusion coefficient of chloride in a free solution [9].

In comparison, the studies of diffuse damage obtained by compression load have shown a marked threshold effect which called percolation threshold, regardless of concrete studied and the experimental protocol adopted to measure the transport properties and crack of concrete [10-17]. If the crack network is not connected, these transport properties are related to the concrete itself, such as the porosity of concrete and interconnectivity of the pore system. Beyond the percolation threshold cracked concrete its related to crack properties, the gas permeability changes very significantly with the increase of damage level: an increase in permeability with several orders of magnitude for damaged concrete can be observed [8,10-13], while chloride penetration is much less affected by cracks [14-17].

Existing experimental data provide some correlation between the material degradation and the permeability of concrete. The same exists for the influence of the concrete degradation on chloride penetration. Moreover very little data are available on the relationship between permeability and chloride diffusion of

concrete damaged by uniaxial compressive loading. The development of microcracks was often represented by compressive load levels, residual load, or cumulative crack length. That is why this study proposes a link between this concrete degradation and damage variable resulting from a reduction in stiffness of the concrete. Thanks to this research work a relationship between permeability and chloride diffusion will be established by introducing this damage variable in the case of concrete damaged by sustained uniaxial loading to simulate a short-term creep phase and to get diffuse damage. One objective of this research was conducted to achieve further information on the influence of microcracks on the gas permeability and chloride diffusion of ordinary concrete (OC) and high performance (HPC). Concrete cylinders were loaded under uniaxial compression between 60% and 90% of the ultimate strength. The time of sustained load is 2 h for each load level, added 1h and 30 min for high load level. A damage variable can be obtained by static and dynamic method. After unloading intrinsic gas permeability was measured using a constant head permeameter, the chloride migration coefficient was evaluated by migration test in steady state conditions, with the same concrete specimen. These measurements allow the comparison between chloride diffusion and gas permeability for similar concrete at similar load levels.

2 EXPERIMENTAL PROGRAM

2.1 Specimen Preparation

Two concrete mixes were made with the same cement CPA-CEM I 52.5: one ordinary concrete (OC) with a water/cement ratio of 0.49 and high performance with a water/cement ratio of 0.32 (HPC), (see Table 1). Concrete cylinders of length 22 cm and diameter 11 cm were prepared from a single batch for each mix. The concrete mixtures were cast in steel molds and compacted using a mechanical vibrator. After casting the cylindrical specimens were stored in a room maintained at 20°C and about 95% relative

humidity (RH) for 24 hours, and were cured in water at 20°C for 1 year. They were stored in air-conditioned room (20°C and RH 50 ± 5%) until testing. The characteristics of these concretes ageing 1 year are shown in Table 2. The open porosity was measured by water saturation.

Table 1: Details of test series and mix proportion

Mix ingredients (kg/m ³)	OC	HPC
Coarse aggregate, 12.5 – 20 mm	777	550
Medium aggregate, 4 – 12.5 mm	415	475
Sand (Boulonnais), 0 – 5 mm	372	407
Sand (Seine), 0 – 4 mm	372	401
Cement CPA-CEM I 52.5	353	461
Plasticizer	-	12.4
Retarder	-	3.3
Total water	172	146
w/c	0.49	0.32

Table 2: Material properties measured at 1 year

	OC	HPC
Module of elasticity (static evaluation) E ₀ (GPa)	51	51
Compressive strength f _c (MPa)	68	92
Open porosity measured by water saturation (%)	11	9.62

All concrete specimens were tested under an axial compressive loading condition (see Figure 1). After unloading concrete discs of 5 cm in thickness were cut off from the central portion of the cylindrical specimens with a diamond blade saw (see Figure 2).

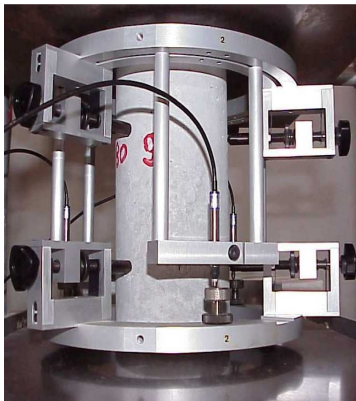


Figure 1: Experimental setup for compressive loading test

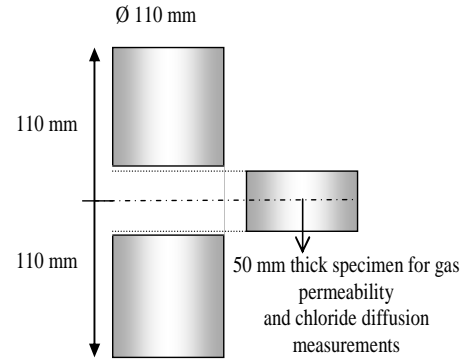


Figure 2: Preparation of the specimen

These discs were sealed with two epoxy resin coats in order to ensure one-dimensional gas and chloride flow through the discs. Drying the discs before proceeding to any gas permeability test is necessary [12,13,18,19]. In this study, all disc specimens are oven-dried at 60°C to constant weight. This procedure has taken 2 months for OC and 3 months for HPC. Then, they are cooled for 48h in a desiccator at 20°C before being tested.

After permeability test the cracked samples were then vacuum saturated in order to measure the chloride diffusion. These were placed in vacuum container with a 2.5 kPa pressure for 4 h. Then, with the vacuum pump still running, the container was filled with water saturated with NaOH (0.025 mol/l) and KOH (0.083 mol/l) in order to immerse the specimen. The vacuum was maintained for 24 h before allowing the air to enter into the container [20]. After this saturation procedure, chloride migration test was driving.

2.2 Uniaxial damage

Concrete cylinders were tested under uniaxial compression between 60% and 90% of the ultimate strength measured at 1 year called f_c (see Table 2). An hydraulic press of 2400 kN capacity was used for this test. On each cylinder, the longitudinal strain is measured using an extensometer cell equipped with three linear variable displacement transducers (LVDT), with a range agreeing within 0.5 mm and an accuracy of 1 μm, (see Figure 1). The transducers are laid every 120° intervals to take into account any asymmetric longitudinal strain. The concrete cylinders

were loaded progressively for predetermined load levels. Each load level was being sustained for varying periods up to two hours (Table 3) to simulate a short-term creep phase [17,21]. The short duration of tests was required to avoid the broken of measurement system in the case of high load level (90% f_c). These displacements are recorded during the loading and unloading phase until the recovery was negligible. The average longitudinal displacement is calculated with the three LVDT measurements.

Table 3: Loading Program

Number of specimens	1	1	1	3
Load level (%)	60	70	80	90
Time of load level (h)	2	2	2	0.5, 1 and 2

2.3 Damage evaluation

Damage, as pointed out by Lemaitre [22], can be measured by a number of means including microscopy (number/density of cracks), ultrasonic waves, density changes and changes in relative amplitude of load and strain. Concrete degradation is interpreted herein with the framework of damage mechanics. We adopted an isotropic scalar measure of damage [23], which derives from a reduction in the stiffness of the material, as in Eq. (1):

$$d = (E_0 - E) / E_0 \quad (1)$$

Where E_0 is the initial modulus of elasticity (Table 2), and E is the final modulus of elasticity obtained for damaged concrete.

The modulus of elasticity can be determined by a static and dynamic evaluation. The static modulus of elasticity is usually calculated with (strength-strain) curve from a plastic-fracturing model [24]. Before each stress level, the initial modulus of elasticity of each cylinder was obtained with the slope of the loading curve calculated from 5% to 30% of the ultimate strength. The final modulus of elasticity for damaged concrete is calculated with the unloading curve also from 5% to 30% of the ultimate strength. .

The dynamic modulus of elasticity of concrete can be determined non destructively

using resonance tests based on measuring the fundamental flexural and torsional frequencies of concrete specimens using a ‘Grindosonic’ apparatus [25]. This last were carried out on concrete cylinders before loading to obtain E_0 and immediately after unloading to obtain E .

2.4 Gas permeability test procedure

An apparatus known as the CEMBUREAU permeameter was used for the determination of permeability [26]. This is a constant head permeameter and nitrogen gas is used as the permeating medium. A pressure difference up to 0.3 MPa can be applied to the specimens in the pressure cells which are sealed by a tightly fitting polyurethane rubber pressing under high pressure (0.7 MPa) against the curved surface. Permeability measurements were made in an air-conditioned room ($20 \pm 1^\circ\text{C}$ and $\text{RH } 50 \pm 5\%$). Each disc was tested with five differential pressures: 0.05, 0.1, 0.15, 0.2 and 0.3 MPa. The volume flow rate through the specimens is measured by means of a soap bubble flow meter. After initiating the percolation of nitrogen through a specimen at a given applied pressure, sufficient time (varying from 40 minutes to several hours) is provided for the establishment of steady state flow before an actual measurement is taken. This condition is verified by taking two measurements separated by a 15 minute time interval. If the two values differ by less than 3%, a steady state flow condition is assumed to be achieved.

The apparent coefficient of permeability k_A (m^2) is calculated from the Hagen-Poiseuille expression Eq. (2) for laminar flow of a compressible fluid through a porous body under steady state conditions [9,18].

$$k_A = (Q/A)(2\mu LP_{atm} / P_i^2 - P_{atm}^2) \quad (2)$$

Where L is the thickness of the sample (m), A is the cross-sectional area (m^2), Q is the gas flow (m^3/s), μ is the coefficient of viscosity ($1.78 \cdot 10^{-5}$ Pa.s for nitrogen gas at 20°C), P_i is the applied absolute pressure or inlet pressure (Pa), and P_{atm} is the atmospheric pressure (Pa).

In fact, the gas percolation through a fine porous body like concrete, can be regarded as

resulting from two flow modes: viscous flow and slip flow or Knudsen flow. Various methods for the calculation of non-viscous flow exist. The most widely used is the relation proposed by Klinkenberg Eq. (3) introducing the concept of an intrinsic coefficient of permeability k_v relative to viscous flow only.

$$k_A = k_v (1 + b/P_{am}) \quad (3)$$

Where P_m is mean gas pressure, $P_m = (P_i + P_{am})/2$, b is the Klinkenberg coefficient (Pa) which is function of the porous body and the infiltrated gas, and k_v is the limiting value of gas permeability when the mean pressure P_m tends towards infinity. The method of determination of k_v consists in measuring k_A at different pressures (P_i) and plotting it against the inverse of the mean pressure ($1/P_m$). The slope of the line leads to the empirical Klinkenberg coefficient b and the origin leads to the intrinsic permeability.

2.5 Steady state migration test

Since diffusion experiments are time-consuming, steady state migration tests were developed to accelerate chloride ions through the concrete [27-29]. Each specimen is placed between the two compartments of a cell where flat silicone circular seals ensure that the system is leaktight (Figure 3). The solutions were made with NaOH (0.025 mol/l) + KOH (0.083 mol/l) in upstream and downstream compartment. NaCl (0.513 mol/l) was added in the upstream solution. A 12 V was applied between the sides of the concrete sample and the test was carried out at temperature $T=20\pm 5^\circ\text{C}$. The downstream solution was titrated with silver nitrate (0.05M). As the flux becomes constant, Nernst-Planck's relation allows to deduce the value of the diffusion coefficient, as seen in Eq. (4):

$$J(x) = -D_e(\partial c/\partial x) + D_e(zFE/RTL)c + cv(x) \quad (4)$$

Where D_e is the diffusion coefficient of concrete (m^2/s), c is the chloride concentration of the upstream compartment (mol/m^3) assumed to be constant, $J(x)$ is the flux of chloride ions ($\text{mol}/(\text{m}^2\text{s})$), z is the chloride ion

valency ($z=1$), F is the Faraday constant ($F = 96480 \text{ J}/(\text{V}\cdot\text{mol})$), E is the actual potential drop between the surfaces of specimen (V), R is the gas constant ($R=8.3144 \text{ J}/(\text{mol}\cdot\text{K})$), T is the absolute temperature (K) and $v(x)$ is the velocity of the solute (m/s). If the concrete is saturated, the velocity of the solute can be neglected. Since the potential drop is $\geq 10V$, ions migrate as a result of the electrical field rather than of the concentration gradient. This insures that the diffusion flow can be neglected in the experiments as shown by Andrade [27]. Eq. (4) can be simplified and then Eq. (5) is obtained:

$$D_e = L/c (RT/zFE) J \quad (5)$$

To establish a steady state, the concentration gradient must be constant during the test. Therefore we have to renew the upstream and downstream solutions frequently. The evolution of current during testing showed a small increase at the beginning of the test and then a stabilisation for all concretes.

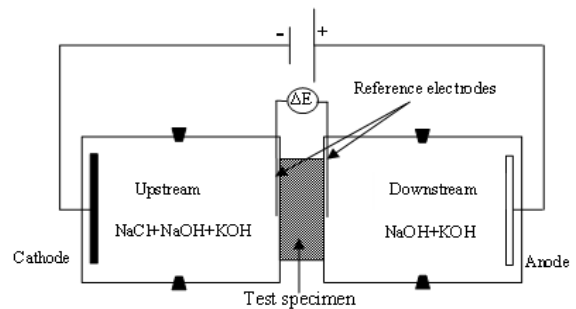


Figure 3: Migration cell

3 RESULTS AND DISCUSSION

3.1 Effect of uniaxial damage on the strain results

Figure 4 presents the evolution of maximal strain ε_{\max} under loading versus load level. The results enhanced that the maximal strain obtained at 2 hours increased regularly with the level of applied load for both concretes. It was generally accepted that the compressive load below $30\%f_c$ will not cause microcracks and thus the crack system remains stable. At $30\%f_c$ to $60\%f_c$ micro cracks in transition zone between the mortar matrix and aggregate

particles begin to increase in length, number, and width as the load increases (as reported in [17,30]). However in these tests, at 60% f_c and above the crack system becomes unstable and continuous due to the rapid propagation of cracks in the concrete. At 90% f_c the maximal strain increased with the increase of the time load. This might be explained by the increase of the crack size due to the expansion of the cylinder and the increase of longitudinal displacement. This result confirms that the cracking pattern is developing during the loading phase only.

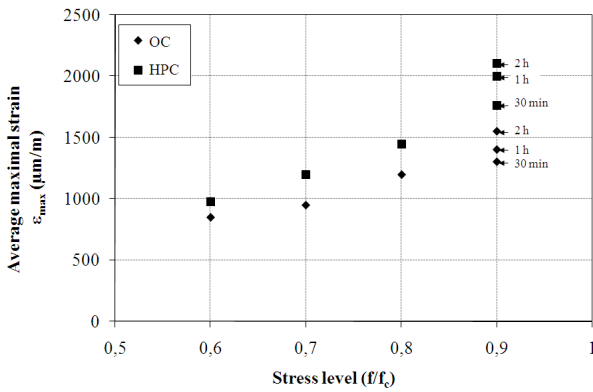


Figure 4: Maximal strain versus stress level

The residual strain ϵ_{res} evaluated after unloading increase linearly with the increase of maximal strain ϵ_{max} for both concretes (see Figure 5).

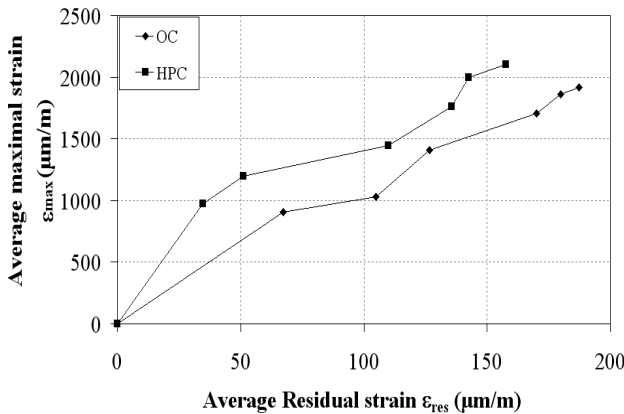


Figure 5: Maximal strain versus residual strain

The microcracking patterns varied among the mixes for each load level the maximal strain under loading of HPC is higher than OC but the residual strain is lower. This implies a

partial closure of the microcracks of HPC concrete after unloading which is due to a more elastic response of HPC than OPC (see Table 2)

3.2 Increase Permeability versus strain

The results obtained from uniaxial damage tests have been used to investigate the damage effect at high load level and its relation with transport properties of concrete (gas permeability and chloride diffusion). Characteristic gas permeability through cracked and uncracked concrete was studied. The concrete under investigation was prepared according to the drying procedures which are given in section 2.1. Gas permeability was then calculated from the volumetric gas flow using Darcy's law for a compressible fluid (Eq. 2.).

The results enhanced that the intrinsic permeability coefficient k_v of OC and HPC increased with the increase of the residual strain, and HPC k_v values were lower than the OC values (Figure 6).

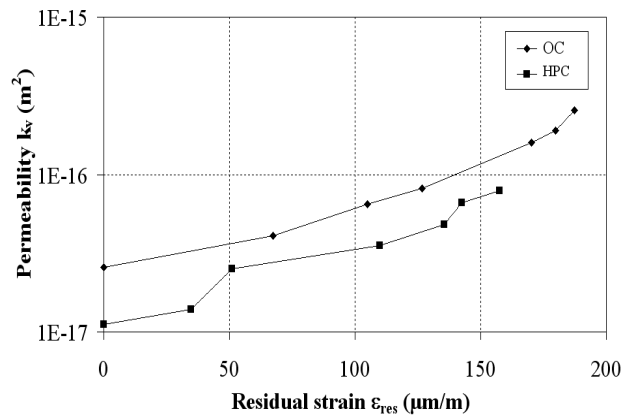


Figure 6: Permeability versus residual strain

This might be explained by the progressive change in the internal structure of the specimen due to the increasing of load level. Concrete is a capillary porous material and its permeability is closely related to its microstructure. The HPC porosity is lower than OC porosity (see Table 2) and thus the HPC gas permeability is lower than OC permeability, the average k_v values for the virgin specimen, were $2,57 \cdot 10^{-17} m^2/s$ for OC and $1,11 \cdot 10^{-17} m^2/s$ for HPC. Once there are

micro cracks in the concrete caused by uniaxial damage, there would also be favourable passages for gas flow, This can be explained by the gas flow through the pores and additionally through cracks in the case of cracked concrete, (as reported in [12,13]). Therefore, higher residual strain would result in higher gas permeability as obtained in figure 6.

3.3 Relationship between increase in gas permeability and damage value

The damage coefficient, d , which is a measure of the stiffness degradation, can be calculated using (Eq. 1). This coefficient was evaluated by both methods (see section 2.3). The first is the static method where the stiffness loss is calculated with the strength/strain curves (as reported in [12,21]). The second is the dynamic method where a reduction of flexural and torsional frequencies of the specimen was observed after unloading measured with the “grindosonic”. For these load levels ($60\%f_c$ to $90\%f_c$), damage coefficients approximately from 0.015 to 0.16 were obtained (see Figure 7).

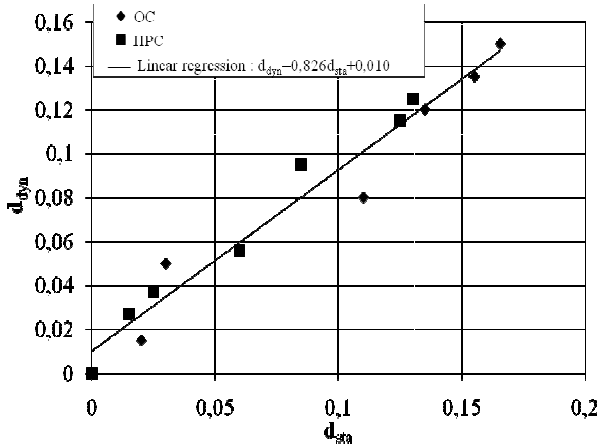


Figure 7: Relationship between damage value obtained by static and dynamic method

The damage coefficient of OC and HPC increased with the increase of the load levels; this is due to the applied load which produces the degradation in the materials shown by a continuous reduction in the elastic modulus and appearance of the residual strain. The damage coefficient evaluated by static or dynamic method of OC is higher than HPC for

the same load level. This result confirms that the crack pattern of OC is more significant than HPC. There is a relationship between the damage variable measured by the static method and that measured by the dynamic method with a correlation coefficient $R^2=0.95$ (Figure 7). This linear relationship shows that the damage obtained by the dynamic method is slightly higher than that obtained by the static method. This linear trend which is non material dependent should be confirmed with others cementitious materials before being used to get damage rate with this very useful non destructive technique.

The relative permeability of cracked concrete $k_v(d)/k_{v0}$ is defined as the ratio between the permeability coefficient of cracked concrete $k_v(d)$ and the permeability coefficient of uncracked concrete k_{v0} . It can be related to the damage variable “ d ”. The increase in permeability relative permeability $k_v(d)/k_{v0}$ with the damage coefficient evaluated by dynamic method is illustrated in Figure 8. $k_v(d)/k_{v0}$ tended to increase slightly beyond the damage coefficient of 0,03 for both concretes.

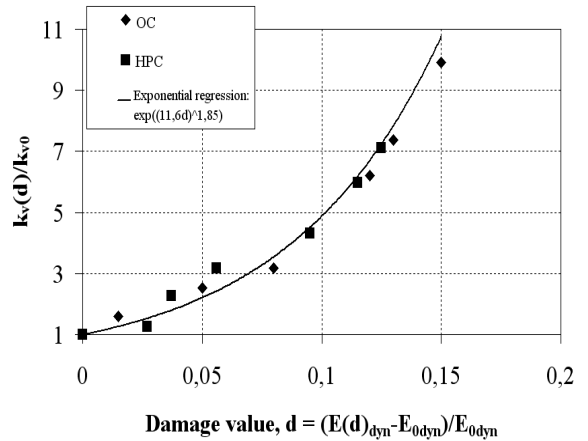


Figure 8: Relation between relative permeability and damage value

This range of damage coefficient corresponds to the observed load level which was found $70\%f_c$ for OC and HPC. An exponential curve for the relative increase of gas permeability was obtained as a function of damage coefficient. A similar relation was obtained by Picandet et al. [12] using cyclic compression test.

3.4 Effect of uniaxial damage on chloride diffusion

After the measurements of the gas permeability on virgin and cracked specimen, these specimens were then saturated in basic solution in order to measure the chloride diffusion. The accumulation of chloride ions in the downstream compartment is shown as a function of time for OC and HPC in Figure 9.

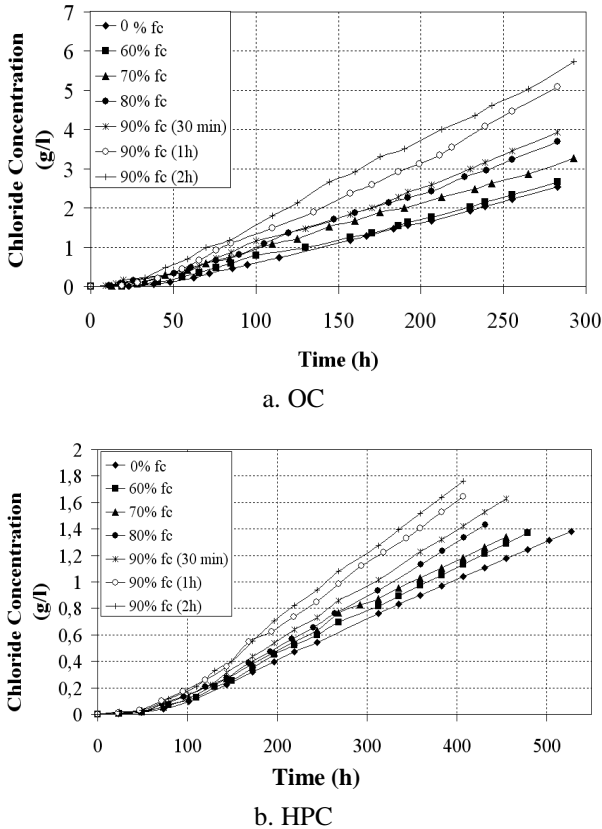


Figure 9: Evolution cumulative increase of chloride in downstream cell

The amount of chloride ions that had flowed through the thickness of the concrete specimen was recorded and plotted versus time and for different load level. The results show a transition period and a steady state period. The transition period was dependent on the concrete mixes and on the microcracks. In steady state period the increase in the amount of chloride ions became linear and the flux J is calculated with the constant slope of a regression line. These slopes were used to calculate the diffusion coefficient of chlorides ions using Eq. (5).

The time to penetrate through the specimen is called lag time (T_{lag}), which is the intersection point of the line with the X-axis [9]. The results showed that for virgin concrete the chloride diffusion coefficient increased with the increase of the porosity, the average diffusion coefficients for the virgin specimen, were $1,88 \cdot 10^{-12} \text{ m}^2/\text{s}$ for OC and $0,67 \cdot 10^{-12} \text{ m}^2/\text{s}$ for HPC. For the applied load of $90\% f_c$ for 2 hours, the diffusion coefficient were $5,74 \cdot 10^{-12} \text{ m}^2/\text{s}$ for OC and $1,28 \cdot 10^{-12} \text{ m}^2/\text{s}$ for HPC. Figure 10 presents the variation of time lag versus the diffusion coefficient. The results show that for virgin concrete T_{lag} of HPC are higher than for OC. A higher T_{lag} may result from a lower porosity. This is an effect of the material. T_{lag} depends on the porosity of concrete and chloride binding [31] However, for cracked specimen it appears that T_{lag} decreased with the diffusion coefficient D_e increasing. A linear correlation was obtained between the diffusion coefficient D_e and the time lag T_{lag} .

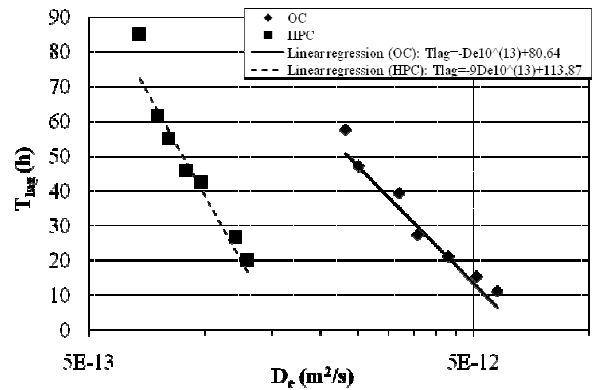


Figure 10: Relation between time lag and diffusion coefficient

The time lag reduction T_{lag} between virgin and most cracked concrete is more marked for HPC which has a T_{lag} of virgin concrete higher than the OC. The Time lag reduction of HPC is about 65h while it's about 47h for OC. This was due probably to chloride ion penetration from microcracks to the virgin concrete, which was considered to occur more easily in OC concrete compared with HPC as OC porosity is higher than HPC porosity. This essentially means that the effect of cracking on T_{lag} is

more important for dense materials with a higher T_{lag} for the uncracked material.

3.5 Increase chloride diffusion coefficient versus strain

The chloride diffusion coefficients evolutions of OC and HPC versus a residual strain are reported in Figure 11. It seems that the diffusion coefficient less sensitive than gas permeability to the residual deformation obtained. This variation begins for residual deformations in excess of 100 μ/m corresponding to loads greater than 70% f_c for OC and 80% f_c for HPC.

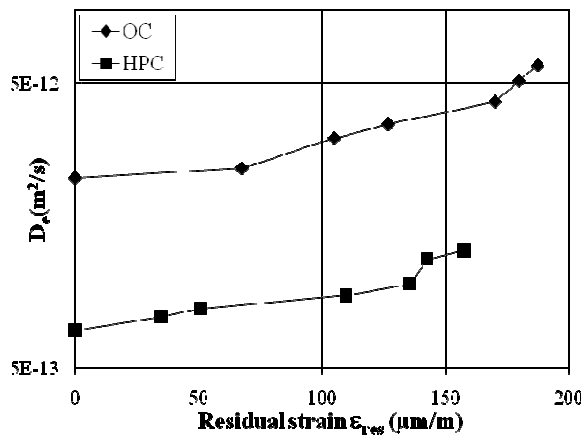


Figure 11: Effect of residual strain on chloride diffusion

3.6 Relationship between increase chloride diffusion coefficient and damage value

The relative diffusivity of cracked concrete $D_c(d)/D_{e0}$ is defined as the ratio between the diffusion coefficient of cracked concrete $D_c(d)$ and the diffusion coefficient of uncracked concrete D_{e0} . It can be related to the damage variable “d”. Figure 12 presents the evolution of relative diffusivity of cracked concrete with damage value assessed by the dynamic method. This evolution which is non material dependant is consistent with an increasing more marked for OC which has a diffusion coefficient of uncracked concrete larger than the HPC. The relative diffusivity of OC for the high load level is about 2.5 while it’s about 2.19 for HPC. From Figure 12 the relationship between these two parameters has an exponential variation with a correlation coefficient $R^2=0.94$. This relationship is

similar to that obtained for the gas permeability with different empirical coefficients. This allows to develop an empirical relationship between these two transfer parameters, even if they are not corresponding to the same transport mechanisms.

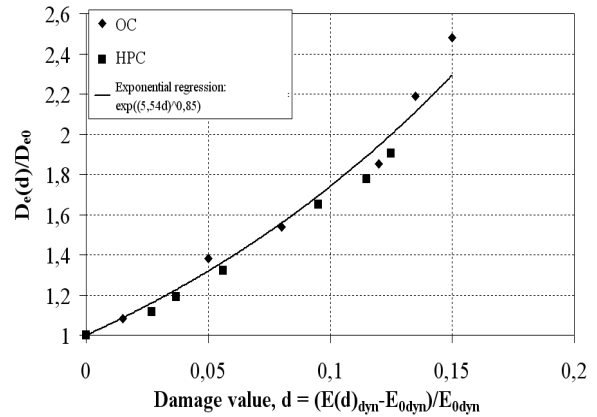


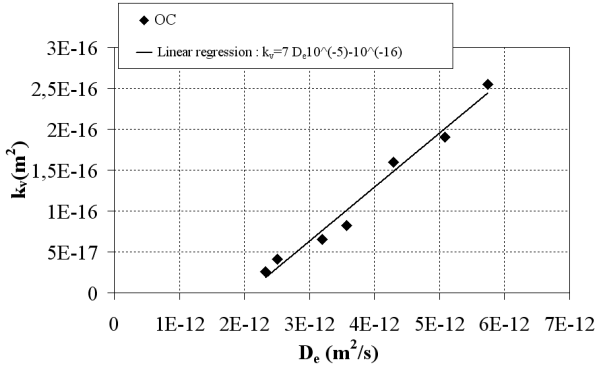
Figure 12: Relation between increase in diffusion coefficient and damage value

3.7 Relationship between increase in the gas permeability and chloride diffusion coefficient

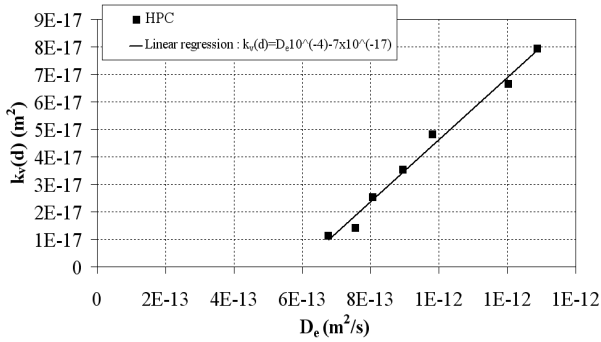
Gas permeability and diffusivity are governed by two transport modes. The variation of these two parameters depends on the microstructure of concrete and cracking that can be characterized by the damage. According to the equations presented in Figure 8 and Figure 12, we find that the gas permeability and diffusion coefficient show a same trend based on the damage variable. This allows us to establish a relationship between these two transfer parameters. Gas permeability is measured on a dry sample as the diffusion coefficient is measured on the same sample in saturated state by migration test under steady state condition. The results show that there is a linear relationship between the evolution of these two parameters depending on the damage variable, specific for each concrete type (Figure 13), with a correlation coefficient $R^2 = 0.98$ for OC and $R^2 = 0.99$ for HPC.

Figure 14 shows the variation of the $k_v(d)/k_{v0}$ according to the ratio $D_c(d)/D_{e0}$ for OC and HPC. The existence of a microcrack

network seems to modify significantly the sustainability indicators. However, the influence is different for each concrete. It is observed that gas permeability is more sensitive to damage: in the case of OC $k_v(d)/k_{v0}$ increases by a factor of 10 while $D_e(d)/D_{e0}$ increases by a factor of 2.5. For high-performance concrete $k_v(d)/k_{v0}$ increases by a factor of 7 while $D_e(d)/D_{e0}$ increases by a factor of 1.9.



a. OC

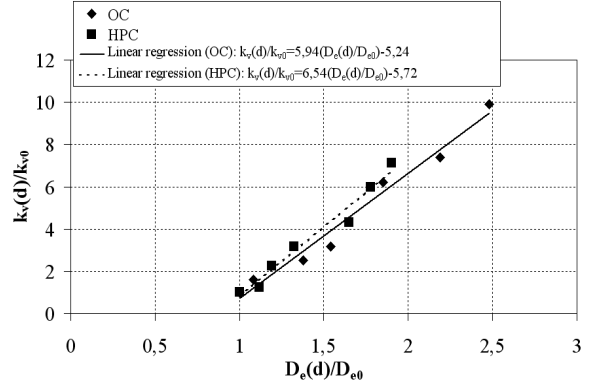


b. HPC

Figure 13: Relationship between chloride diffusion and gas permeability

It is noted that the relative permeability increases linearly with the relative diffusion coefficient, with a correlation coefficient $R^2 = 0.98$ for OC and $R^2 = 0.97$ for HPC. This relation could be assimilated to a no material dependant linear relationship. This could be useful to avoid experimental test: only gas permeability are request to calculate the relative diffusion coefficient of cracked concrete. The increase obtained for these two transfer parameters is more important for OC than for HPC, this result confirms that micro cracking obtained with diffuse damage impact on the transfer parameters for concrete which

have higher porosities. Cracking contributes to the increase in the total porosity of the material and causes a change in the distribution of pore size [32]. The increased connectivity of cracks is more important for concrete which has the highest porosity.


Figure 14: Comparison between relative permeability and relative chloride diffusion coefficient

4 CONCLUSIONS

From the results presented in this paper it can be concluded that:

The diffuse damage of concrete can be obtained using a uniaxial compression test. For loads above $60\%f_c$, the maximal strain ϵ_{max} and residual strain $\epsilon_{rés}$ increase with increasing load and time load for both concretes OC and HPC. This variation can be interpreted by the existence of microcracks and their evolution according to the applied load.

The diffuse damage obtained by uniaxial compression test in pre-peak affects the diffusion of chloride ions. This damage causes an increase in the diffusion coefficient D_e and a decrease in the time lag T_{lag} . There is a linear correlation between these two parameters; this relationship is specific for each of concrete type. The effect of cracking on reduction of time lag T_{lag} is different than on the increase of the relative diffusivity $D_e(d)/D_{e0}$. The reduction of T_{lag} is more pronounced on HPC than OC, whereas the increase of the relative diffusivity $D_e(d)/D_{e0}$ is more marked for OC than for HPC. This can be explain by transport process of chloride ions in cracked concrete, for the same load level the penetration of chloride ions through the cracked sample is easily for HPC compared to the OC but with a

flow low than OC. This results in an increase of the relative diffusivity for OC than for HPC and reduced T_{lag} for dense concrete.

A linear correlation is obtained between intrinsic permeability coefficient k_v and diffusion coefficient D_e depending on the damage variable, specific for each concrete type (OC and HPC). The increase of these two transfer parameters is greater for OC than for HPC. This type of damage assigns more particularly the concrete that have a higher porosity.

Gas permeability is more sensitive of concrete damage than chloride diffusion: in the case of OC $k_v(d)/k_{v0}$ increases by a factor of 10 while $D_e(d)/D_{e0}$ increases by a factor of 2.5. For high-performance concrete $k_v(d)/k_{v0}$ increases by a factor of 7 while $D_e(d)/D_{e0}$ increases by a factor of 1.9.

REFERENCES

- [1] Sugiyama, T., 1996. Determination of chloride diffusion coefficient and gas permeability of concrete and their relationship. *Cement and Concrete Research* **26**:781-790.
- [2] Maage, M., Helland, S., Poulsen, E., Vennesland, O., and Carl, J.E., 1996. Service life prediction of existing concrete structures exposed to marine environment. *ACI Materials Journal* **93**:602-608.
- [3] Jung, W.Y., Yoon, Y.S., Sohn, Y.M., 2003. Predicting the remaining service life of land concrete by steel corrosion. *Cement and Concrete Research* **33**:663-677.
- [4] Zhang, W.M., Ba., H.J., 2011. Accelerate life test of concrete in chloride environment. *Journal of materials in civil Engineering* **23**:330-334.
- [5] Picandet, V., Khelidj, A., Bellegou, H., 2009. Crack effect on gas and water permeability of concretes. *Cement and Concrete Research* **39**:537-547.
- [6] Aldea, C., Shah, P., Karr, A., 1999. Effect of cracking on water and chloride permeability of concrete. *Journal of materials in civil Engineering* **11**:181-187.
- [7] Olga, GR., Doug Hooton, R., 2003. Influence of cracks on chloride ingress into concrete. *ACI Materials Journal* **100**:120-126.
- [8] Tognazzi, C., Ollivier, J.P., Carcasses, M., Torrenti, J.M., 1998. Couplage fissuration-dégradation chimique des matériaux cimentaires: premiers résultats sur les propriétés de transfert. In : Petit, Pijauder Cabot, Reynouard (Eds), *Ouvrage Géomatériaux et interactions-Modélisations Multi-Echelles*, Hermes, France.
- [9] Djerbi, A., Bonnet, S., Khelidj, A., Baroghel-bouny, V., 2008. Influence of traversing crack on chloride diffusion into concrete. *Cement and Concrete Research* **38**:877-883.
- [10] Kermani, A., 1991. Permeability of stressed concrete. *Building Research and Information* **19**:362-365.
- [11] Sugiyama, T., 1996. Effect of stress on Gas permeability in concrete. *ACI Materials Journal* **93**:443-450.
- [12] Picandet, V., Khelidj, A., Bastian, G., 2001. Effect of axial compressive damage on gas permeability of ordinary and high-performance concrete. *Cement and Concrete Research* **31**:1525-1532.
- [13] Choinska, M., Khelidj, A., Chatzigeorgiou, G., Pijaudier-Cabot, G., 2007. Effects and interactions of temperature and stress-level related damage on permeability of concrete. *Cement and Concrete Research*, **37**: 79-88
- [14] Sugiyama, T., 1994. Permeability of stressed concrete. Doctoral thesis, Dept. of Civil Engineering, University of new Brunswick, Canada.

- [15] Samaha, H.R., 1992. Influence of microcracking on the mass transport properties of concrete. *ACI Materials Journal* **89**:416-424.
- [16] Saito, M., 1995. Chloride permeability of concrete under static and repeated loading. *Cement and Concrete Research* **25**:803-808.
- [17] Lim, C., 2000. Microcracking and chloride permeability of concrete under uniaxial compression. *Cement and Concrete Composite* **22**:353-360.
- [18] Jacobs, F., 1998. Permeability to gas of partially saturated concrete. *Magazine and Concrete Research* **50**:115-121
- [19] Nagataki, S., 1980. Effect of heating condition on air permeability of concrete at elevated temperature. *Transaction of the Japanese Concrete Institute* **10**:147-154.
- [20] Méthodes recommandées pour la mesure des grandeurs associées à la durabilité, 1998. Proceedings of Journées Technique APC-AFREM, *Durabilité des Bétons*, France,
- [21] Mazzotti, C., Savoia, M., 2002. Non linear Creep, Poisson's Ratio, and Creep-Damage interaction of Concrete in Compression. *ACI Materials Journal* **99**:450-457.
- [22] Lemaitre, J., Dufailly, J., 1987. Damage measurements. *Engineering Fracture Mechanics*, **28**:643-661.
- [23] Jessen, S.M., Plumtree, A., 1989. Fatigue damage accumulation in pultruded glass/polyester rods, *Composites* **20**:559-567.
- [24] Mazars, J., 1984. Application de la mécanique de l'endommagement au comportement non linéaire et à la rupture du béton de structure. Doctoral thesis, E.N.S.E.T., Université Pierre et Marie Curie, C.N.R.S.
- [25] Allison, R.J., 1987. Non-destructive determination of Young's modulus and its relationship with compressive strength, porosity and density, *Geological Society of London Special Publication* **29**:3-69.
- [26] Kollek, J.J., 1989. The determination of the permeability of concrete to oxygen by the Cembureau method – a recommendation, *Materials and Structures* **22**:225-230.
- [27] Andrade, C., 1993. Calculation of chloride diffusion coefficient in concrete from ionic diffusion measurements. *Cement and Concrete Research* **23**: 724-742.
- [28] Truc, O., 2000. A new way for determining the chloride diffusion coefficient in concrete from steady state diffusion test. *Cement and Concrete Research* **30**:217-226.
- [29] Luping, T., 1996. Chloride transport in concrete-Measurement and predictions. Doctoral thesis, Dept. of Building Materials, Chalmers University of Technology, Gothenburg, Sweden.
- [30] Smadi, M.M., Slate F.O., 1989. Microcracking of high and normal strength concretes under short and long term loadings. *ACI Material Journal* **86**:117-127.
- [31] Bigas, J-P, 1994. La diffusion des ions chlore dans les mortiers. Doctoral thesis, INSA de Toulouse.
- [32] Baroghel-Bouny, V., 1994. Caractérisation des pâtes de ciment et des bétons ; méthodes, analyse, interprétations. *Edition du Laboratoire Central des Ponts et Chaussées*, Paris, France.